JCSE The Journal of Corrosion Science and Engineering
ISSN 1466-8858 Volume 20, Preprint 64 first submitted 24 May 2017

Studies on the green inhibition of steel corrosion in acid medium

S.Karthikeyan *, P.A.Jeeva , K.Raja
Centre for Innovative Manufacturing Research, VIT University, Vellore, Tamilnadu, India.

(*Corresponding author: skarthikeyanphd@yahoo.co.in)

Abstract

Corrosion behaviour of mild steel in 2M Phosphoric acid with Tinidazole as corrosion inhibitor has been studied by using weight loss, Potentiodynamic polarization, electrochemical impedance spectroscopy, Hydrogen permeation and diffuse reflectance spectroscopic studies. All these techniques reveal that inhibition efficiency increases with the increase in the concentration of inhibitor. Polarization studies indicated that inhibitor behaved as cathodic inhibitor. Diffuse reflectance spectroscopy confirmed the adsorption of inhibitor on the mild steel surface obeying Langmuir adsorption isotherm. A Gaussian simulation technique was used to track the quantum mechanical analysis and recognized correlations between different types of descriptors and measured corrosion inhibition efficiency for inhibitor. The quantum chemical analysis demonstrates the inhibition efficiencies of the compound determined by electrochemical methods.

Keywords: Mild Steel, Corrosion Inhibition, Tinidazole, Adsorption Isotherm, Quantum chemical studies.

1. Introduction

Mild steel is an important category of metals due to its excellent mechanical properties. It is extensively used under different conditions in chemical and allied industries in handling acidic, alkaline and salt solutions. Mild is used in industries as pipelines for petroleum industries, storage tanks, reaction vessel and chemical batteries [1]. Acid solutions are widely used in many industrial processes. Acids are used for acid cleaning, pickling and descaling due to their chemical properties [2-5]. Acids cause damage to the substrate, because of their corrosive nature. Several methods were used to decrease the corrosion of metals in acidic medium, but the use of inhibitors is most commonly used [6-10].

ISSN 1466-8858 Volume 20, Preprint 64 first submitted 24 May 2017

Organic compounds are widely used as corrosion inhibitors for mild steel in acidic media [11-16]. The rate of corrosion decreases by adsorption of organic inhibitors on the metal surface. The inhibitors block the active sites by displacing water molecules and form a compact barrier film on the metal surface. The most of the organic inhibitors are toxic, highly expensive and non environment friendly. Research activities in recent times are geared towards developing the cheap, non-toxic drugs as environment friendly corrosion inhibitors [17-21].

The aim of this work is to investigate the corrosion protection efficiency of Tinidazole for mild steel corrosion in 2M H_3PO_4. We came to know that exceedingly few reports are available by using this compound as corrosion inhibitor in 0.1M H_2SO_4 [22-24]. No concrete report is available for the use these compounds as corrosion inhibitors in 1M H_3PO_4. From the literature the higher concentration of H_3PO_4 acts as pickling solution for mild steel for electroplating, battery electrodes using sulphur containing organic compounds. Use of this inhibitor in 2M H_3PO_4 will reduce the metal loss in acid medium. The compound is large enough and sufficiently planar to block more surface area on the mild steel. The inhibition efficiency was calculated using weight loss measurement, potentiodynamic polarization studies, impedance techniques, hydrogen permeation studies and diffuse reflectance methods. A definite correlation exists between different types of descriptors and measured corrosion inhibition efficiency for Tinidazole using chemical and electrochemical techniques.

2. Experimental Details

2.1. Materials

Mild steel specimens of size 1x4 cm^2 were used for weight loss and electrochemical studies. The aggressive solution of 2M H_3PO_4 (AR Grade) was used for all the studies. The antibiotic namely Tinidazole was purchased from the corresponding manufacturing company. The structure of the antibiotic is given in the figure 1. Electrochemical experiments were performed using a three electrode cell assembly with mild steel samples as working electrode, 4cm^2 area of platinum as counter electrode and $Hg/Hg_2Cl_2/KCl$ as the reference electrode. The surfaces of corroded and corrosion inhibited mild steel specimens were examined by diffuse reflectance studies in the region 200-700 nm using U-3400 spectrometer (UV-VIS-NIR Spectrometer, Hitachi, Japan).

JCSE The Journal of Corrosion Science and Engineering
ISSN 1466-8858 Volume 20, Preprint 64 first submitted 24 May 2017

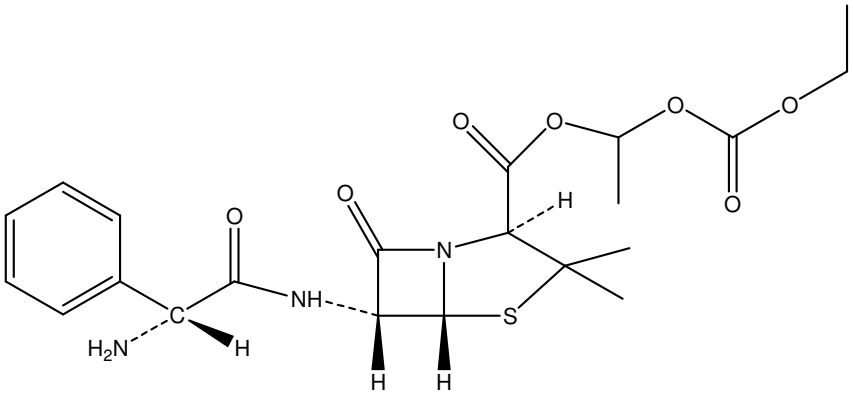

Fig.1: Structure of Tinidazole

2.2. Weight loss studies

The concentrations of inhibitor used for weight loss and electrochemical study were from $2x10^{-4}M$ to $20x10^{-4}M$. Mild steel specimens of size 1x4 cm^2 were abraded with different emery papers and washed with acetone. The cleaned samples were then washed with double distilled water and finally dried and kept in the desiccator. The weight loss study was carried out at room temperature for three hours in 2M H_3PO_4. The inhibition efficiency (IE %) was determined by the following equation

$$\text{Inhibition Efficiency (IE \%)} = (W_0 - W_i / W_0) \times 100$$

Where W_0 & W_i are the weight loss values in the absence and presence of the inhibitor.

2.3. Electrochemical studies

Potentiodynamic polarization measurements were carried out in a conventional three electrode cylindrical glass cell, using CH electrochemical analyzer. The solution was deaerated for 15 minutes before carryout the polarization studies. The working electrode was maintained at its corrosion potential for 10 min. until a steady state was obtained. The mild steel surface was exposed to various concentrations of inhibitors in 100mL of 1M H_3PO_4 at room temperature. The inhibition efficiency (IE %) was calculated using the equation.

$$\text{Inhibition Efficiency (IE \%)} = (I_0 - I / I_0) \times 100$$

ISSN 1466-8858 Volume 20, Preprint 64 first submitted 24 May 2017

Where I_0 and I are the corrosion current density without and with the inhibitor respectively.

The potentiodynamic current-potential curves were recorded by changing the electrode potential automatically from -750mV to +150mV versus the open circuit potential. The corresponding corrosion current (I_{corr}) was recorded. Tafel plots were constructed by plotting E versus log I. Corrosion Potential (E_{corr}), corrosion current density (I_{corr}) and cathodic and anodic slopes (β_c and β_a) were calculated according to known procedures.

Impedance measurements were carried out in the frequency range from 0.1 to 10000 Hz using amplitude of 20 mV and 10 mV peak to peak with an AC signal at the open-circuit potential. The impedance diagrams were plotted in the nyquist representation. Charge transfer resistence (R_{ct}) and double layer capacitance (C_{dl}) values were obtained from nyquist plot [25, 26]. The percentage inhibition efficiency was calculated from the equation

$$\text{Inhibition Efficiency (IE \%)} = (R_{ct} - R'_{ct} / R_{ct}) \times 100$$

Where R'_{ct} and R_{ct} are the corrosion current of mild steel with and without inhibitor respectively.

2.4. Hydrogen permeation studies

The hydrogen permeation study was carried out using an adaptation of modified Devanathan and Stachurski's , two compartment cell as described elsewhere [27]. Hydrogen permeation current was recorded in the absence and presence of inhibitors.

2.5. Diffuse reflectance spectroscopy

The surfaces of corroded and corrosion inhibited mild steel specimens were examined by diffuse reflectance studies in the region 200- 700 nm using U-3400 spectrometer [UV-VIS-NIR Spectrometer, Hitachi, Japan].

2.6. Theoretical calculations

Quantum calculations were carried using MOPAC 2000 program of CS Chemoffice packet program. The energy of highest occupied molecular orbital (HOMO), lowest unoccupied molecular orbital (LUMO), Dipole moment (μ), hardness, absolute softness and total energy of the molecule were calculated with the above given software package.

JCSE The Journal of Corrosion Science and Engineering
ISSN 1466-8858 Volume 20, Preprint 64 first submitted 24 May 2017

3. Results and discussion

3.1. Weight loss studies

The values of inhibition efficiency (IE %), corrosion rate (CR) and surface coverage (θ) calculated for Tinidazole in 2M H_3PO_4 at different concentrations from the weight loss data are summarized in the table-1. It is obvious that inhibition efficiency enhances with increase in the inhibitor concentration. In addition the rate of corrosion has reduced with increase in inhibitor concentration. Maximum inhibition efficiency is obtained at $45x10^{-3}$ M concentrations of the inhibitor.

Table 1. Weight loss parameters for the corrosion of mild steel immersed in 2M phosphoric acid in presence of different concentrations of Tinidazole

Inhibitor Conc. (M)	Inhibition Efficiency	Surface Coverage [θ]
Blank	-	-
$15x10^{-3}$	71.47	0.7147
$30x10^{-3}$	88.68	0.8868
$45x10^{-3}$	97.72	0.9772

3.2. Potentiodynamic polarization studies

Polarization curves for mild steel in 2M H_3PO_4 containing different concentrations of inhibitor are given in figure-2. The values of corrosion potential (E_{corr}) , corrosion current densities (I_{corr}), anodic tafel slope (β_a) ,cathodic tafel slope (β_c) surface coverage(θ) and inhibition efficiency (IE%) calculated using polarization curves are summarized in table-2.

JCSE The Journal of Corrosion Science and Engineering
ISSN 1466-8858 Volume 20, Preprint 64 first submitted 24 May 2017

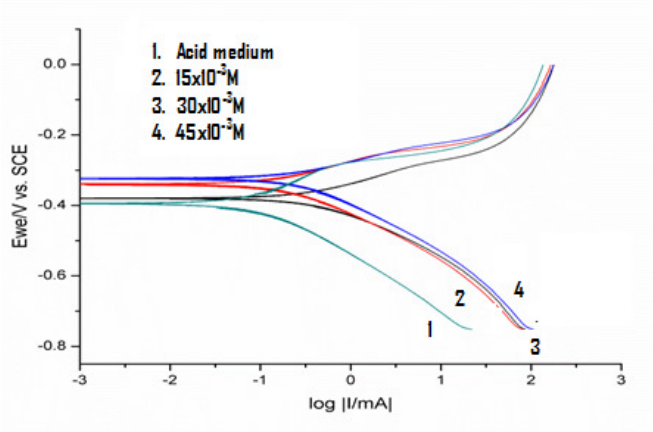

Fig 2. Polarization curves of mild steel recorded in 2M H_3PO_4 in presence of different concentrations of Tinidazole

According to the results, corrosion current (I_{corr}) value decreases with increase in the concentration of the inhibitor. The inhibition efficiency (IE %) and surface coverage (θ) increases with increase in inhibitor concentration. The maximum inhibition efficiency is achieved at $45x10^{-3}$ M concentration. Both β_a and β_c are reduced, but the values of β_c are decreased to a greater extent. This indicates that the compound behave as cathodic inhibitor.

ISSN 1466-8858 Volume 20, Preprint 64 first submitted 24 May 2017

Table 2: Potentiodynamic polarization parameters for mild steel immersed in 2M H_3PO_4 in the presence of different concentrations of Tinidazole.

Inhibitor Con. [M]	E_{corr} [mV vs SCE]	I_{corr} [μA cm^{-2}]	β_a [mV dec^{-1}]	β_c [mV dec^{-1}]	Inhibiton efficiency [%]	Surface coverage [θ]
Blank	-397.55	572.00	84.5	140.8	-	-
$15x10^{-3}$	-387.62	163.36	70.2	137.3	71.44	0.7144
$30x10^{-3}$	-323.18	65.09	59.7	133.02	88.62	0.8862
$45x10^{-3}$	-311.55	13.15	47.22	80.7	97.70	0.9770

3.3. Electrochemical impedance studies

The Nyquist representations of impedance performance of mild steel in 2M H_3PO_4 with and without addition of different concentrations of Tinidazole are shown in the figure-3. A large capacitive circle at higher frequency range is observed at all concentrations of the inhibitor. The higher frequency capacitive loop is due to the adsorption of inhibitor molecule [28].

JCSE The Journal of Corrosion Science and Engineering
ISSN 1466-8858 Volume 20, Preprint 64 first submitted 24 May 2017

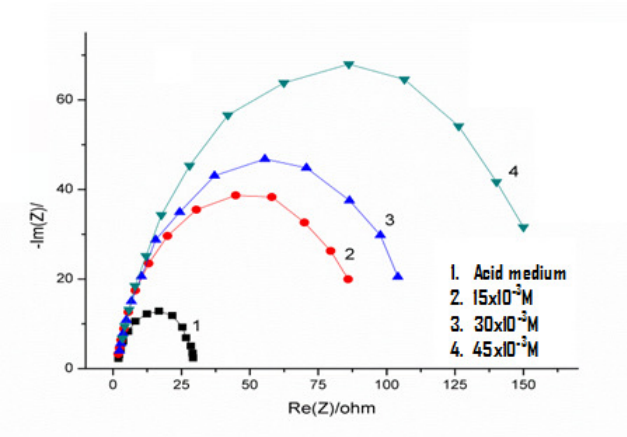

Fig. 3: Nyquist plot for mild steel immersed in 2M H_3PO_4 containing different concentrations of Tinidazole

Values of charge transfer resistance (R_{ct}) and double layer capacitance (C_{dl}) derived from Nyquist plots are shown in table 3. The values of R_{ct} are found to increase with increase in concentration of inhibitor in 2M H_3PO_4. It is found that values of C_{dl} are fetched down by increasing concentrations of inhibitor in the acid. This can be ascribed to the well-built adsorption of the compounds on the metal surface.

Table 3: Electrochemical impedance parameters for mild steel immersed in 2M H_3PO_4 in the presence and absence of different concentrations of Tinidazole.

Inhibitor Con. [M]	R_{ct} [Ω cm²]	C_{dl} [F cm⁻²]	Inhibition efficiency [%]	Surface coverage[θ]
Blank	33.2	0.530	-	-
15x10⁻³	102.3	0.151	71.44	0.7144
30x10⁻³	114.4	0.060	88.66	0.8866
45x10⁻³	168.65	0.012	97.72	0.9772

ISSN 1466-8858 Volume 20, Preprint 64 first submitted 24 May 2017

3.4. UV spectral reflectance studies

The reflectance curves for polished specimen, specimen dipped in 2M H_3PO_4 and various concentrations of inhibitor are given in the figure.4. The percentage of reflectance is highest for polished mild steel and it steadily reduces for the specimen dipped in 2M H_3PO_4 solution. This observation discloses that the change in surface feature is due to the corrosion of mild steel in acid. The reflectance percentage of steel in the presence of inhibitor is higher than steel as immersed in blank. This validates that the surface property of steel are not altered further due to the formation of film on the metal. The reflectance percentage decreases with increase in thickness of the inhibitor film formed on metal surface. Similar observation has been made by Madhavan et al [29].

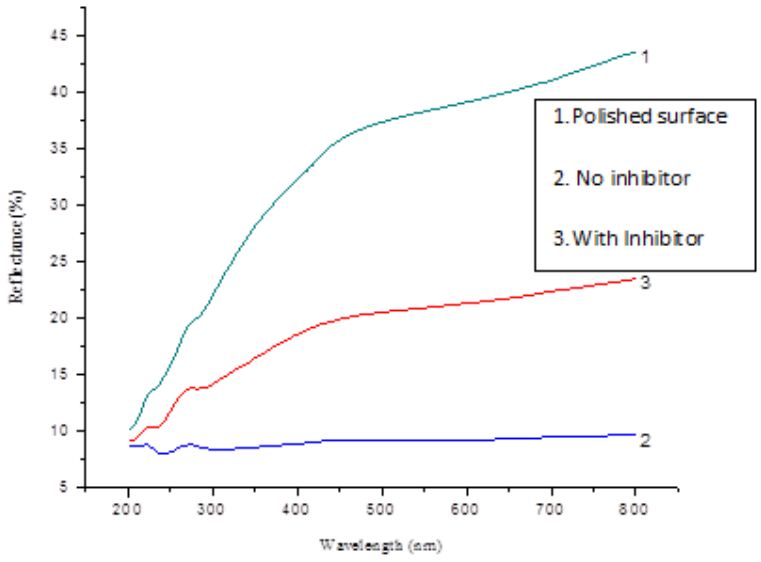

Fig. 4: UV Reflectance curves of mild steel in 2M H_3PO_4 solution with $20x10^{-4}$M concentration of the inhibitor.

3.5. Adsorption isotherm and thermodynamic parameters

The inhibitive action of inhibitor in highly aggressive media is due to its adsorption on the metal surface. The degree of surface Coverage (θ) for different concentrations of inhibitor in 2M H_3PO_4 has been calculated from weight loss, Polarization and Electrochemical Impedance studies. The acquired data was tested graphically for fitting suitable isotherm [30-32]. Almost a straight line was obtained by plotting log (C/θ) Vs

ISSN 1466-8858 Volume 20, Preprint 64 first submitted 24 May 2017

log C as shown in Figure-5, which proves that the adsorption of these compounds on steel surface obeys Langmuir adsorption isotherm.

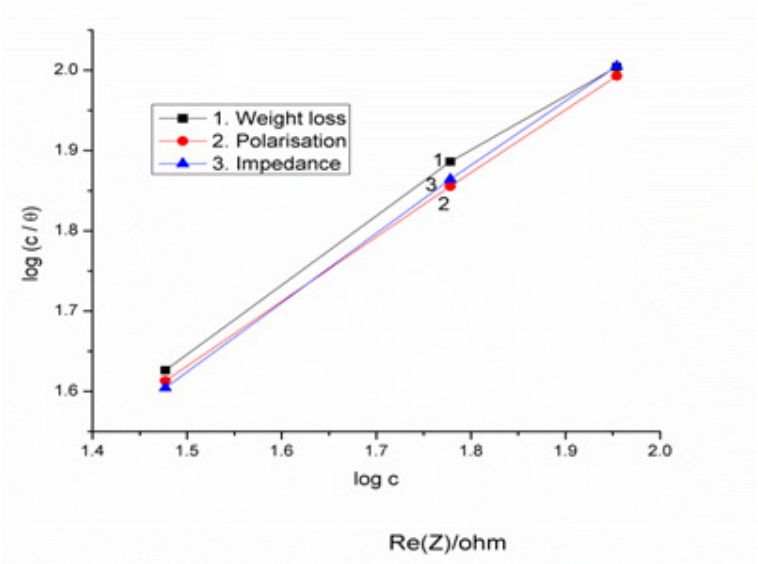

Fig. 5: Langmuir's adsorption isotherm plots for the adsorption Tinidazole in 2M H_3PO_4 on the surface of mild steel.

The Langmuir isotherm for the adsorbed layers is given by the equation [33],

$$C_{inh}/\theta = 1/K_{ads} + C_{inh}$$

Where K_{ads} is the equilibrium constant of the adsorption/desorption process. Adsorption equilibrium constant [K_{ads}] and free energy of adsorption [ΔG^0_{ads}] were calculated using the equation [34]

$$K_{ads} = 1/C_{inh} \times \theta/1-\theta$$

$$\Delta G^0_{ads} = -2.303RT \log [55.5K_{ads}]$$

Where 55.5 is the molar concentration of water in solution [35]. R is the gas constant, T is the temperature. The values of adsorption equilibrium constant [K_{ads}] and free energy of adsorption [ΔG^0_{ads}] are given in table-4. The negative values of [ΔG^0_{ads}] pointed out that adsorption of inhibitors is spontaneous process. It is reported that values of [ΔG^0_{ads}] is of

ISSN 1466-8858 Volume 20, Preprint 64 first submitted 24 May 2017

order 20 kJmol^{-1} or lower indicates a physisorption, those of order of -40 kJmol^{-1} or higher involve charge sharing or transfer from the inhibitor to the metal surface specifies a chemisorptions [36-38]. The values of free energy of adsorption [ΔG^0_{ads}] in our experiment lies in the range -28 to -32 kJmol^{-1}, demonstrating that the adsorption is not a simple physisorption, but it may involve some other interactions [39].

Table 4: Gibbs free energy parameters and adsorption equilibrium constant [K] of inhibitor at various temperatures evaluated by weight loss method.

Temperature (K)	K_{ads}	$-\Delta G^0_{ads}$ (kJmol^{-1})
313	954	28.30
323	1191	29.80
333	1372	31.11

3.6. Hydrogen permeation measurements

Hydrogen permeation currents are recorded in H_3PO_4 in the absence and presence of inhibitor. This study has been taken up with a plan of selecting the inhibitor with a view to their efficacy on the reduction of hydrogen uptake [40]. The values of permeation current with respect to time are given in table-5. Figure 6 shows the variation of permeation current vs time for mild steel in 2M H_3PO_4 in the presence of Tinidazole.

ISSN 1466-8858 Volume 20, Preprint 64 first submitted 24 May 2017

Table 5: Values of permeation current for mild steel in 2M H_3PO_4 and in presence of inhibitors with respect to change in time

	Permeation Current (μA)	
Time (min.)	2M H_3PO_4	Tinidazole
0	10.2	2.7
5	11.4	4.1
10	12.3	4.9
15	12.1	5.4
20	13.4	6.2
25	13.4	6.2
30	13.4	6.2
35	13.4	6.2
40	13.4	6.2

The Tinidazole reduces the permeation current to the extent of 53%. The corrosion inhibition efficiency of the compound in 2M H_3PO_4 follows the same fashion . Thus a definite correlation is noticed between the corrosion inhibition efficiency and the extent of reduction in the permeation current of the compound. It is a recognized fact that higher β_c value for an inhibiting compound, the lesser is the corrosion and hydrogen ingress on the metal. An increase in the β_c value, favours to increase in the energy barrier for proton discharge and reduction in the evolution of hydrogen. This in turn leads to lower permeation of hydrogen through the mild steel.

JCSE The Journal of Corrosion Science and Engineering
ISSN 1466-8858 Volume 20, Preprint 64 first submitted 24 May 2017

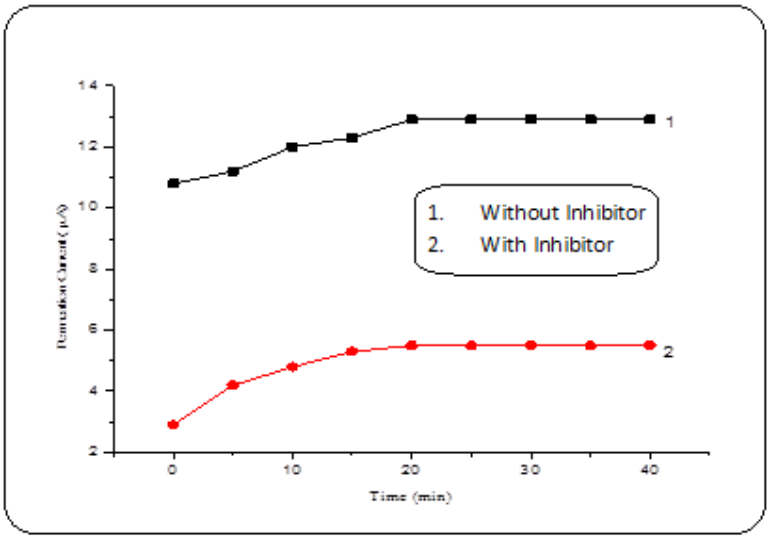

Fig.6: Hydrogen permeation Vs Time curves for mild steel immersed in 2M H_3PO_4 and $45x10^{-3}$ M concentration of inhibitor

3.7. Mechanism of corrosion inhibition

The adsorption of Tinidazole on the mild steel surface is found to be majorly physical in nature. Physical adsorption is a process of electrostatic attraction between charged species in the solution and the metal surface. If the metal surface is positively charged, the adsorption of negatively charged species is facilitated. Positively charged species can also adsorb on the positively charged metal surface with the help of negatively charged intermediate, which adsorb first on the positively charged metal surface and allows positively charged species to adsorb on it.

Thus the adsorption of Tinidazole may take place in two different ways as

(i) The sulphoxide group of Tinidazole may hinder the adsorption of inhibitor on steel .However the delocalized electrons of nitrogen atoms may release electrons which favours the adsorption of Tinidazole on steel surface.

(ii) The inhibitor may compete with acid anions for the adsorption sites at the water covered surface on steel and adsorb by donating electrons to the mild steel surface [41, 42].

ISSN 1466-8858 Volume 20, Preprint 64 first submitted 24 May 2017

3.8. Quantum chemical calculations

Quantum chemical calculations were carried out to investigate the adsorption and inhibition mechanism of the inhibitors. Figure 7 shows the optimized structure of Tinidazole. The values of calculated quantum chemical parameters i.e. E_{HOMO} (highest occupied molecular orbital), E_{LUMO} (lowest unoccupied molecular orbital), ΔE (energy gap), μ (dipole moment), σ (softness) etc. are summarized in table-6.

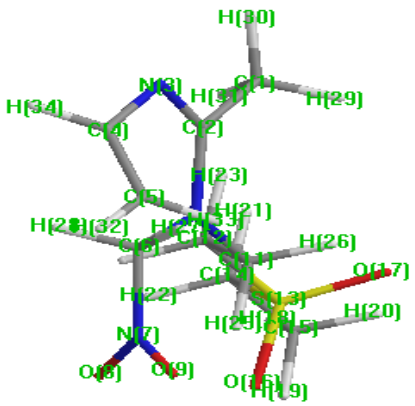

Fig. 7: Optimized structure of Tinidazole

E_{HOMO} is associated with the electron-donating ability of the molecule. Several researchers have shown that the adsorption of an inhibitor on metal surface can occur on the basis of donor-acceptor interactions between the π-electrons of heterocyclic atoms and the vacant d-orbitals of the metal surface atoms [43-45]. A high value of E_{HOMO} indicates a tendency of a molecule to donate electrons to acceptor molecules with low energy empty molecular orbital. Increasing values of E_{HOMO} facilitates the adsorption and increases the inhibition efficiency by influencing the transport process through the adsorbed layer [46]. E_{LUMO} indicates the ability of the molecule to accept the electrons, hence these are acceptor states. The lower the value of E_{LUMO}, the more probable is that the molecule can accept electrons and increase the inhibition efficiency. Regarding ΔE (E_{LUMO}-E_{HOMO}) lower values of energy difference will cause higher inhibition efficiency because energy to release electron from last occupied orbital will be low. When dipole moment is concerned higher values of μ, will favours a strong interaction of inhibitor molecule with the metal surface [47].

ISSN 1466-8858 Volume 20, Preprint 64 first submitted 24 May 2017

Other indicators are absolute electro negativity (χ), absolute hardness (η). Absolute electro negativity is a chemical property that describes the ability of a molecule to attract electron towards itself in a covalent bond. Absolute hardness is measured by the energy gap between E_{HOMO} and E_{LUMO}. Absolute softness σ is the reciprocal of the hardness. χ, η, σ are calculated using the energies of HOMO and LUMO orbital's of the inhibitor molecules are related to the ionization potential (I), electron affinity (A) by the following relations

$$\chi = I + A/\ 2,\ \eta = I - A\ /\ 2,\ \sigma = 2\ /\ I - A$$

$$\text{Where } I = -E_{HOMO},\quad A = -E_{LUMO}$$

The results deduced indicate that the electron flow will happen from the molecule with low electro negativity towards that of higher value until the chemical potentials are same. In our studies the best inhibition effect is shown by Tinidazole with low electro negativity.

Table 6: Quantum mechanical parameters for Tinidazole for the corrosion of mild steel inphosphoric acid medium.

Inhibitor	LUMO (eV)	HOMO (eV)	ΔE (Cal.Mol-1)	Dipole moment (Debye)
Tinidazole	-1.29664	-2.2984	1.0017	3.1

The higher value of dipole moment and lower total energy for Tinidazole indicates the strong interaction of inhibitor with metal that leading to improved adsorption. The nitrogen atom exerts +M effect on Tinidazole, leads to enhanced corrosion inhibition.

From figure 8 it can be observed that the energy highly occupied molecular orbital's (HOMO) are localized on hetero atoms for Tinidazole.

JCSE The Journal of Corrosion Science and Engineering
ISSN 1466-8858 Volume 20, Preprint 64 first submitted 24 May 2017

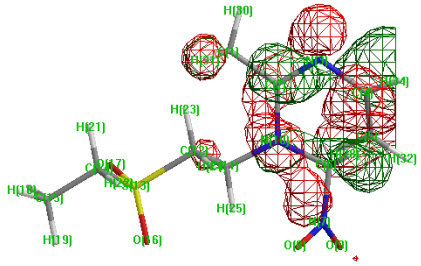

Fig.8: The Highest occupied molecular orbital of Tinidazole

From Figure 9 it is observed that lowest unoccupied molecular orbital's (LUMO) of Tinidazole, which is responsible for its better adsorption of the inhibitor on steel surface than Ampicillin and its allied derivatives.

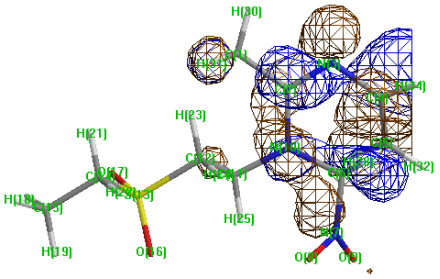

Fig. 9: The lowest unoccupied molecular orbital of Tinidazole

4. Conclusions

1. The use of antibiotic viz., Tinidazole as corrosion inhibitor in 2M H_3PO_4 was systematically studied using weight loss, potentiodynamic polarization, impedance measurements and hydrogen permeation studies.

ISSN 1466-8858 Volume 20, Preprint 64 first submitted 24 May 2017

2. The adsorption of inhibitor on mild steel surface follows Langmuir adsorption isotherm. The adsorption of inhibitor on steel surface is further justified by diffuse reflectance spectra results.

3. The quantum mechanical studies validate the performance of antibiotic as potential corrosion inhibitor for mild steel in 2M H_3PO_4.

References

1. Zhang J, Liu J, Yu W, Yan Y, You L and Liu L , *Corros.Sci.*, **52,** 6, pp2059-2065, 2010.

2. Obot I B, Obi-Egbedi N O and Umoren S A, *Int. J. Electrochem. Sci.*, **4,** 6, pp-863-877, 2009.

3. Vishwanatham S and Anil Kumar, *Corros. Rev.*, **23,** pp-181-186, 2005.

4. Eddy N O, Ebenso E E and Ibok U J, *J. Appl. Electrochem*. **40,** 2, pp445-456, 2010.

5. Ebenso E E, Alemu H, Umoren S A and Obot I B, *Int. J. Electrochem. Sci.*, **3,** pp1325-1339, 2008.

6. Shukla S K, Quraishi M A and Prakash R, *Corros. Sci.*, **50,** 10, pp2867-2872, 2008.

7. Ranney M W, Inhibitors—Manufacture and Technology; Noyes Data Corp: NJ, 1976.

8. Singh A K, Shukla S K, Singh M and Quraishi M A, Mater. Chem. Phys. 129, 1, pp68-76, 2011.

9. Shukla S K and Quraishi M A, *Mater.Chem. Phys.*, **120,** 2, pp-142-147, 2010.

10. Eddy N O and Ebenso E E, *Afri J of Pure & Appl Chem*, **2,** 6, pp46-54, 2008.

11. Lagrenee M, Mernari B, Bouanis M, Traisnel M and Bentiss F, *Corros Sci*, **44,** 3, pp573-588,2002.

12. Quraishi M A and Khan S, *J Appl Electrochem*, **36,** 5, pp539-544, 2006.

ISSN 1466-8858 Volume 20, Preprint 64 first submitted 24 May 2017

13. Quraishi M A, Athar M and Ali H, *Br Corros J*, **37,** pp155-158, 2002.

14. Hasanov R, Sadikoglu M and S. Bilgic, *Appl. Surf. Sci.*, **253,** pp3913-3921, 2007.

15. Chetouani A, Hammouti B, Benhadda T and Daoudi M, *Appl. Surf. Sci.*, **249,** 1, pp375-385, 2005.

16. Bouklah M, Hammouti B, Lagrenee M and Bentiss F, *Corros. Sci.*, **48,** 9, pp2831-2842, 2006.

17. Abdallah M, *Corros Sci* , **44,** 4, pp717-728, 2002.

18. Abdallah M, *Corros Sci* , **46,** 8, pp1981-1996, 2004.

19. El-Naggar M M , *Corros Sci* , **49,** 5, pp2226-2236, 2004.

20. Solmaz R , Kardas G , Yazici B and Erbil M, *Protection of Metals* , **41,** 6, pp581-585, 2005.

21. Sing W T, Lee C L ,Yeo S L, Lim S P, Sim M M, *Bioorg Med Chem Lett.*, **11,** 2, pp91-94, 2001.

22. Nnabuk O. Eddy, Eno E. Ebenso and Udo J. Ibok , *J Appl Electrochem*, **40,** 2, pp445-456, 2010.

23. Nnabuk O. Eddy, Udo J. Ibok , Eno E. Ebenso, Ahmed El Nemr and El Sayed H.ElAshry, *J Mol Model*, **15,** 9, pp1085-11092, 2009.

24. Nnabuk O E, Siaka A A, Atiku A F and Muhmmad A *Innovations in Science and Engineering,* **1,** pp-79, 2011.

25. Bentiss F, Lagrenee M, Traisnel M and Hornez JC, *Corros Sci.*, **41,** 4, pp789-803, 1999.

ISSN 1466-8858 Volume 20, Preprint 64 first submitted 24 May 2017

26. Ashassi-Sorkhabi H, Shaabani B and Seifzadeh D, *Electrochim Acta*, **50,** 16, pp3446-3452, 2005.

27. Devanathan M A V and Stachurski Z, *Proc.Roy.Soc.*, **270 A,** pp-90, 1962.

28. Shukla S K and Quraishi M A, *Corros. Sci*. doi:10.1016/j.corros.2009.05.020, 2009.

29. Madhavan K, Quaraishi M A, Karthikeyan S and Venkatakrishna Iyer S, *J.Electrochem. Soc. India*, **49,** pp-183, 2000.

30. Ayse Ongun Yuce and Gulfeza Kardas, *Corros Sci.*, **58,** pp86-94, 2012.

31. Eddy N O and Ebenso E E, *E-Journal of Chemistry*, **7,** S1, pp-S442-S448, 2010.

32. Eddy N O, Odoemelam S A and Mbaba A J, *African Journal of Pure and Applied Chemistry* , **2, 12,** pp132-138, 2008.

33. Lebrini M, Traisnel M, Lagrenee M, Mernari B and Bentiss F, *Corros. Sci*. **50,** 2, pp473-479, 2008.

34. Morad M S and Kamal El-Dean A M, *Corros. Sci.*, **48,** 11, pp3398-3412, 2006.

35. Tang L , Mu G and Liu G, *Corros. Sci.*, **45,** 10, pp2251-2262, 2003.

36. Khamis E, Bellucci F, Latanision R M and El-Ashry E S H, Corrosion, 47, 9, pp677-686, 1991.

37. Geler E and Azambuja D S, *Corros. Sci.*, **42,** 4, pp631-643, 2000.

38. Abiola O K, *Corros. Sci*. **48,** pp3078-3090, 2006.

39. Singh A K and Quaraishi M A, *Corros. Sci*. **52,** 4, pp1529-1535, 2010.

40. Madhavan K, Karthikeyan S and Venkatakrishna Iyer S, J.Electrochem Soc.India, **50,** pp-37, 2001.

41. Dehr I and Ozcan M, *Mater. Chem. Phys*. **98,** pp-316, 2006.

ISSN 1466-8858 Volume 20, Preprint 64 first submitted 24 May 2017

42. Keles H, Keles M, Dehri I and Serindag O, *Mater. Chem. Phys.,* **112,** pp173-179, 2008.

43. Ju H, Kai Z P and Li Y, *Corros. Sci.*, **50,** 3, pp865-871, 2008.

44. Issa R M, Awad M K and Atlam F M, *Appl.Surf.Sci.*, **255** pp2433-2441, 2008.

45. Khaled K F and Al-Qahtani M M, *Mater. Chem. Phys.*, **113,**pp150-158, 2009.

46. Laarej K, Bouachrine M, Radi S, Kertit S and Hammouti B, *E-Journal of Chemistry*, **7, 2,** pp419-424, 2010.

47. Ambrish Singh, Quraishi M A, Avyaya J N, and Eno. E. Ebenso, *Res Chem Intermed.*, DOI 10.1007/s11164-012-0577-y, 2012.